(19) **United States**

(12) **Patent Application Publication** (10) Pub. No.: **US 2018/0244521 A1**

Yao et al. (43) Pub. Date: **Aug. 30, 2018**

(54) **METHOD FOR SPLITTING CARBON DIOXIDE INTO MOLECULAR OXYGEN AND CARBON**

(71) Applicant: **California Institute of Technology**, Pasadena, CA (US)

(72) Inventors: **Yunxi Yao**, Pasadena, CA (US); **Konstantinos P. Giapis**, Pasadena, CA (US)

(73) Assignee: **California Institute of Technology**, Pasadena, CA (US)

(21) Appl. No.: **15/905,708**

(22) Filed: **Feb. 26, 2018**

Related U.S. Application Data

(60) Provisional application No. 62/463,021, filed on Feb. 24, 2017.

Publication Classification

(51) **Int. Cl.**
C01B 13/02	(2006.01)
C01B 32/05	(2006.01)
G21K 5/04	(2006.01)

(52) **U.S. Cl.**
CPC *C01B 13/0203* (2013.01); *H05H 5/00* (2013.01); *G21K 5/04* (2013.01); *C01B 32/05* (2017.08)

(57) **ABSTRACT**

Apparatus and methods for facilitating an intramolecular reaction that occurs in single collisions of CO_2 molecules (or their derivatives amenable to controllable acceleration, such as CO_2^+ ions) with a solid surface, such that molecular oxygen (or its relevant analogs, e.g., O_2^+ and O_2^- ions) is directly produced are provided. The reaction is driven by kinetic energy and is independent of surface composition and temperature. The methods and apparatus may be used to remove CO_2 from Earth's atmosphere, while, in other embodiments, the methods and apparatus may be used to prevent the atmosphere's contamination with CO_2 emissions. In yet other embodiments, the methods and apparatus may be used to obtain molecular oxygen in CO_2-rich environments, such as to facilitate exploration of extraterrestrial bodies with CO_2-rich atmospheres (e.g. Mars).
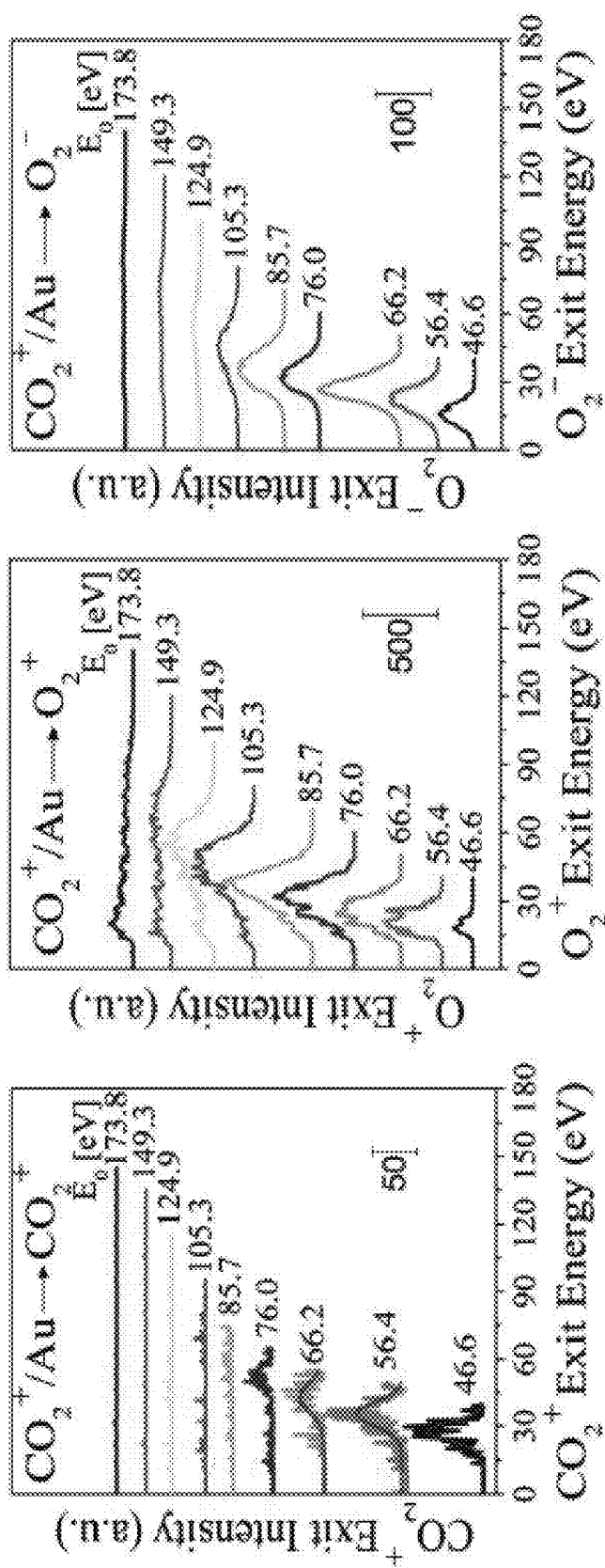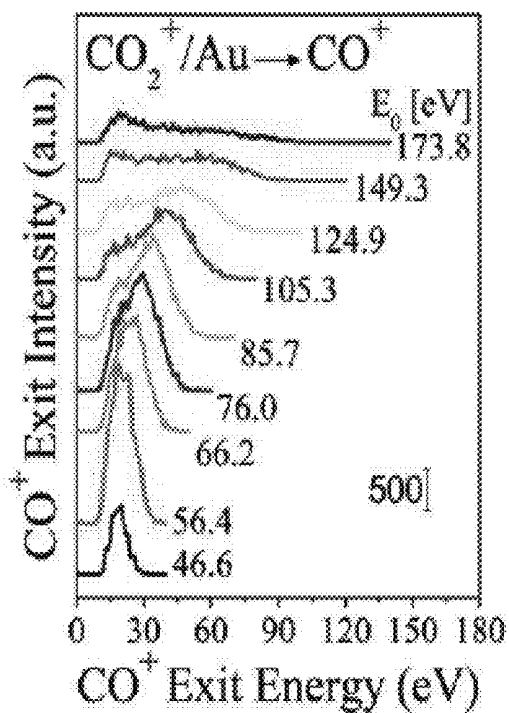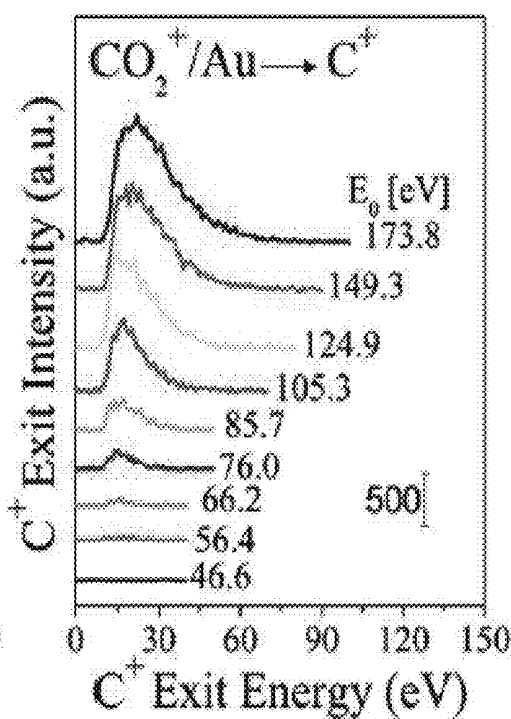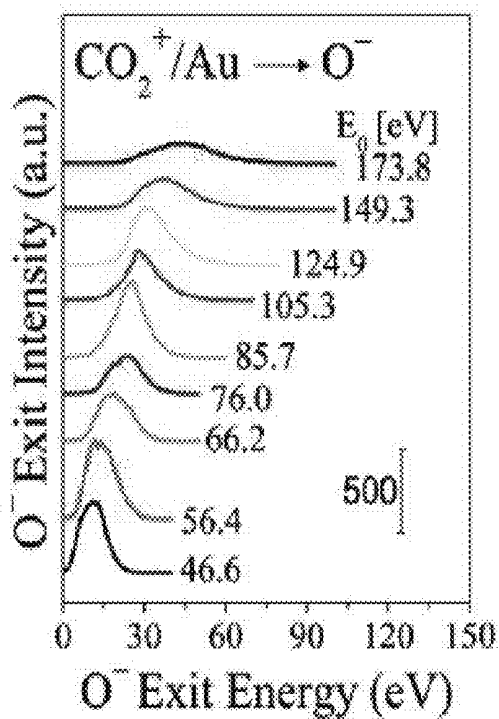
FIG. 1a

FIG. 1b

FIG. 1c

FIG. 2a

$CO_2^+/Au \rightarrow CO^+$

E_0 [eV]
173.8
149.3
124.9
105.3
85.7
76.0
66.2
56.4
46.6

500

CO^+ Exit Intensity (a.u.)

CO^+ Exit Energy (eV)

0 30 60 90 120 150 180

FIG. 2b

$CO_2^+/Au \rightarrow O^+$

E_0 [eV]
173.8
149.3
124.9
105.3
85.7
76.0
66.2
56.4
46.6

500

O^+ Exit Intensity (a.u.)

O^+ Exit Energy (eV)

0 30 60 90 120 150

FIG. 2c

$CO_2^+/Au \rightarrow O^-$

E_0 [eV]
173.8
149.3
124.9
105.3
85.7
76.0
66.2
56.4
46.6

500

O^- Exit Intensity (a.u.)

O^- Exit Energy (eV)

0 30 60 90 120 150

FIG. 2d

$CO_2^+/Au \rightarrow C^+$

E_0 [eV]
173.8
149.3
124.9
105.3
85.7
76.0
66.2
56.4
46.6
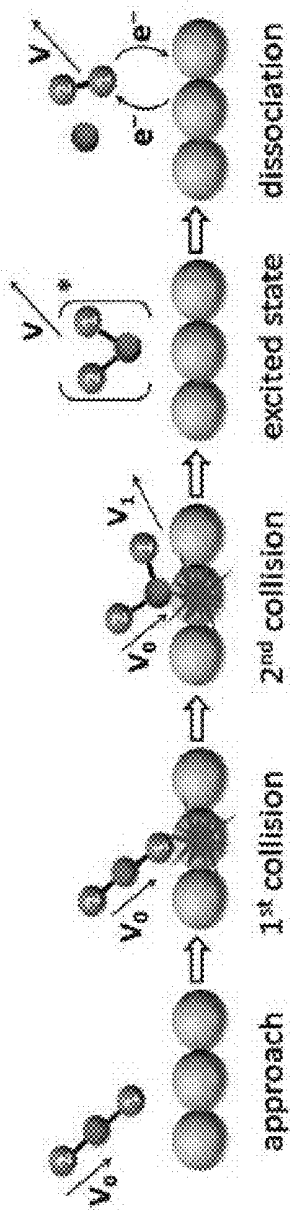
500

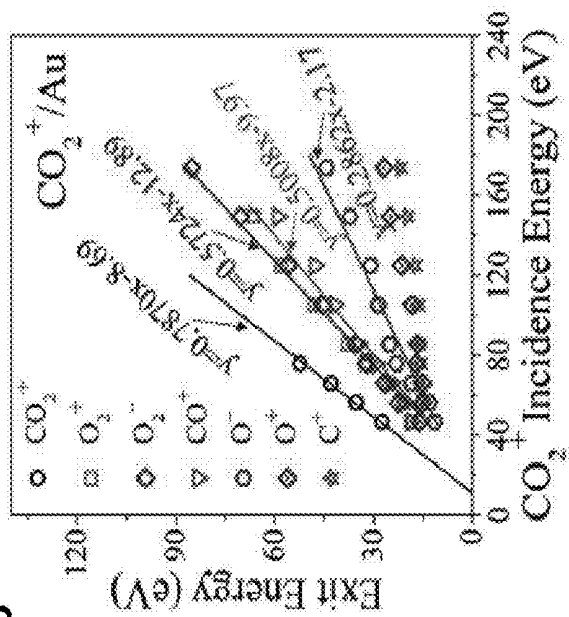C^+ Exit Intensity (a.u.)
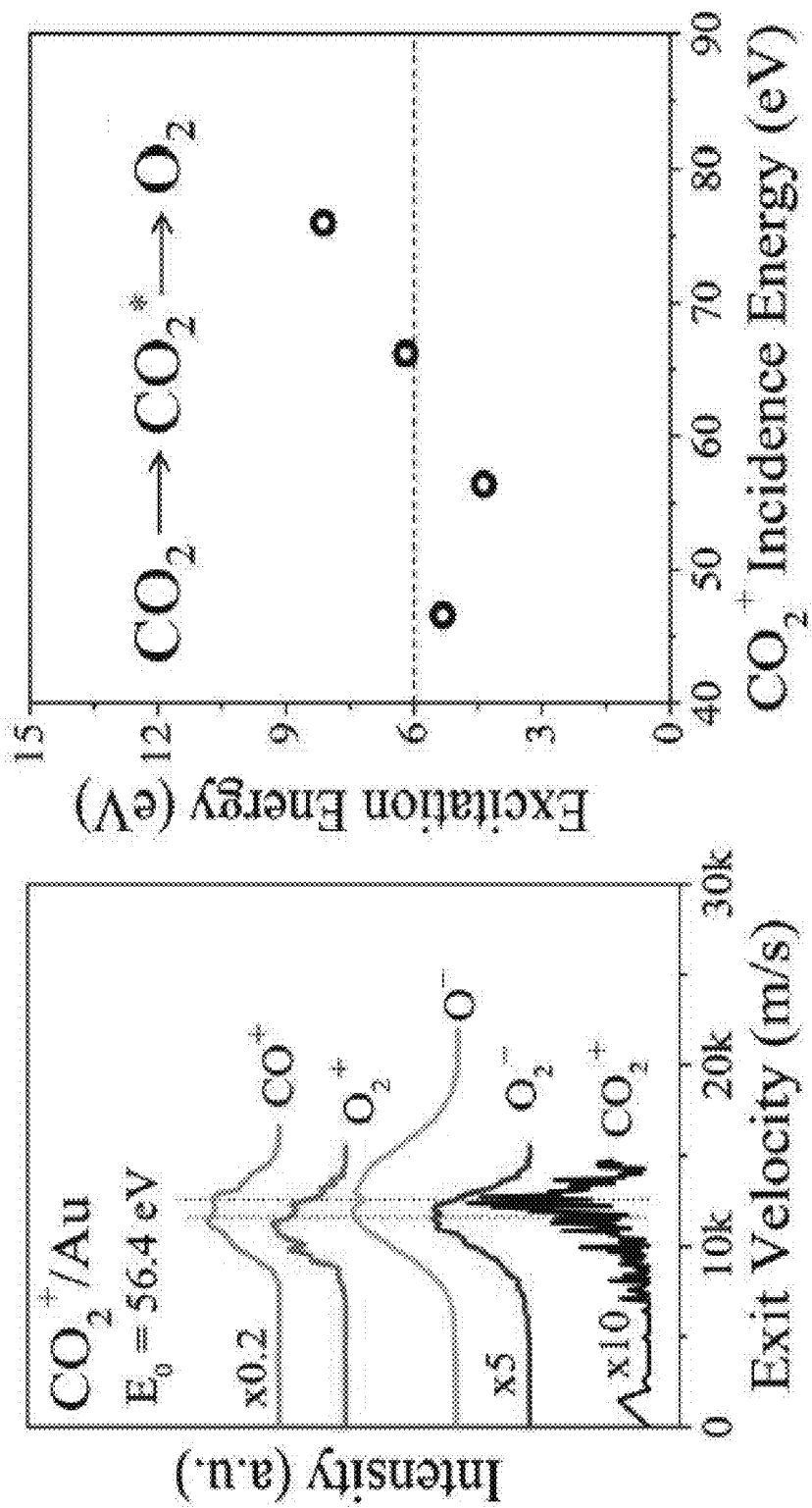
C^+ Exit Energy (eV)

0 30 60 90 120 150

FIG. 3a

FIG. 3b

FIG. 4b

FIG. 4a

FIG. 5

FIG. 6a

FIG. 6b

FIG. 6c

FIG. 7a

$CO_2^+/Pt \rightarrow CO^+$

CO^+ Exit Intensity (a.u.)

E_0 [eV]
130.3
110.7
91.2
81.4
71.6
61.8
52.1

500

0 20 40 60 80 100 120 140
CO^+ Exit Energy (eV)

FIG. 7b

$CO_2^+/Pt \rightarrow O^+$

O^+ Exit Intensity (a.u.)

E_0 [eV]
130.3
110.7
91.2
81.4
71.6
61.8
52.1

500

0 20 40 60 80 100 120
O^+ Exit Energy (eV)

FIG. 7c

$CO_2^+/Pt \rightarrow O^-$

O^- Exit Intensity (a.u.)

E_0 [eV]
130.3
110.7
91.2
81.4
71.6
61.8
52.1

200

0 20 40 60 80 100 120
O^- Exit Energy (eV)

FIG. 7d

$CO_2^+/Pt \rightarrow C^+$

C^+ Exit Intensity (a.u.)

E_0 [eV]
130.3
110.7
91.2
81.4
71.6
61.8
52.1

500

0 20 40 60 80 100 120
C^+ Exit Energy (eV)
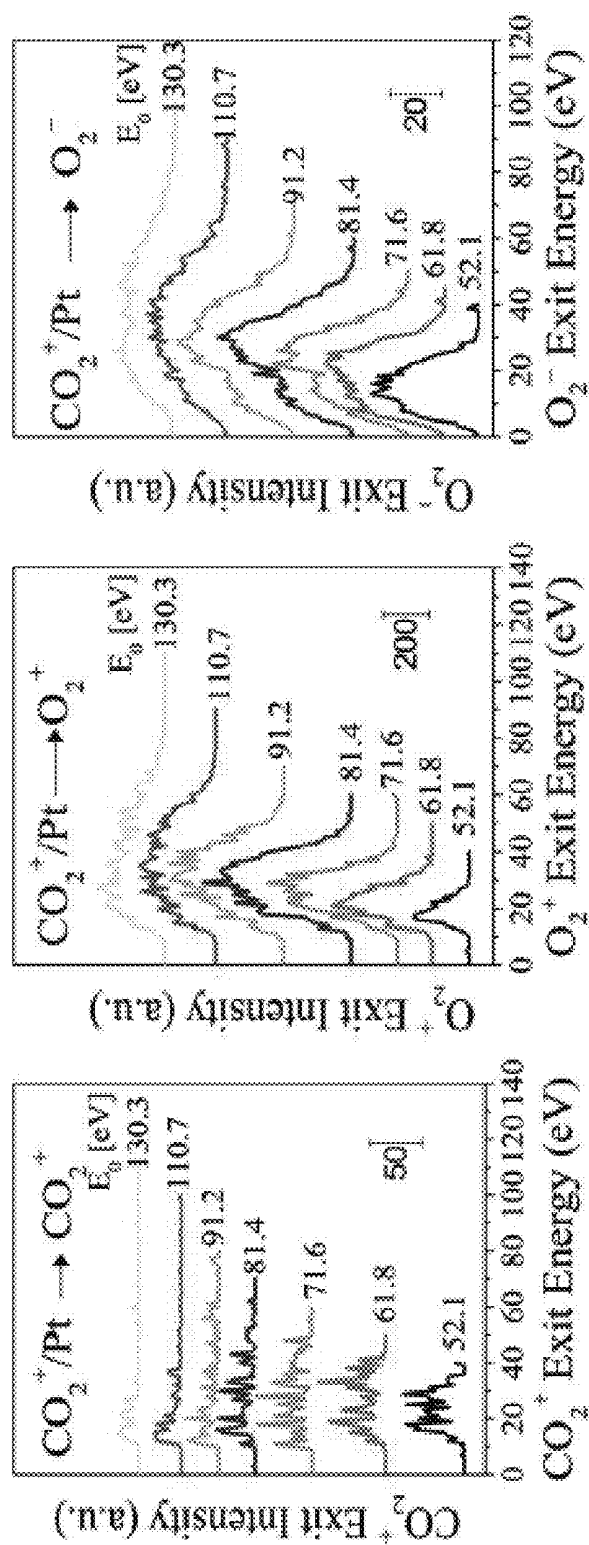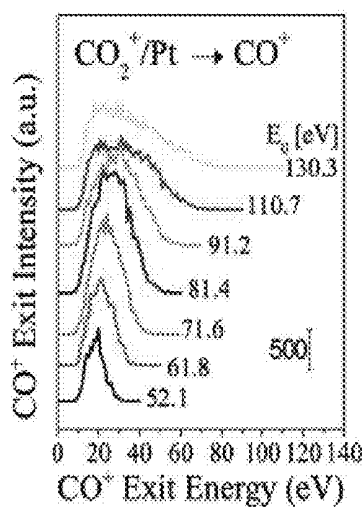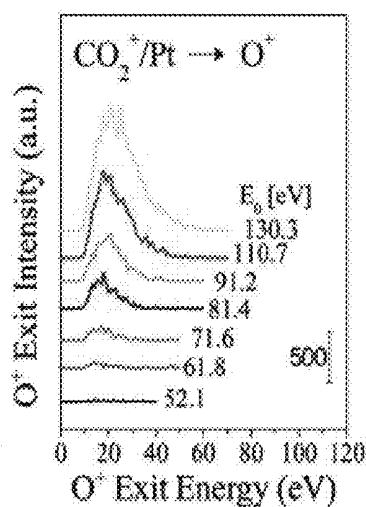
FIG. 8

METHOD FOR SPLITTING CARBON DIOXIDE INTO MOLECULAR OXYGEN AND CARBON

CROSS-REFERENCE TO RELATED APPLICATIONS

[0001] The application claims priority to U.S. Provisional Application No. 62/463,021, filed Feb. 24, 2017, entitled "Method for Splitting Carbon Dioxide into Molecule Oxygen and Carbon," the disclosure of which is incorporated herein by reference.
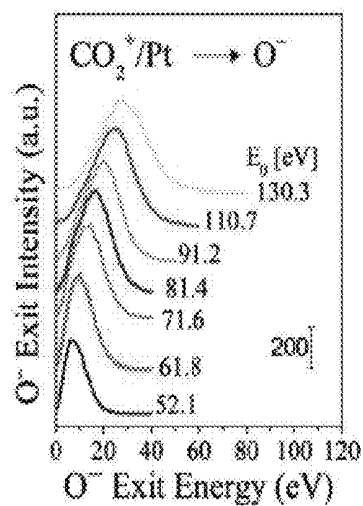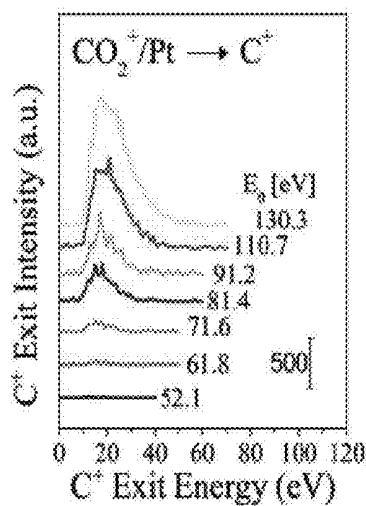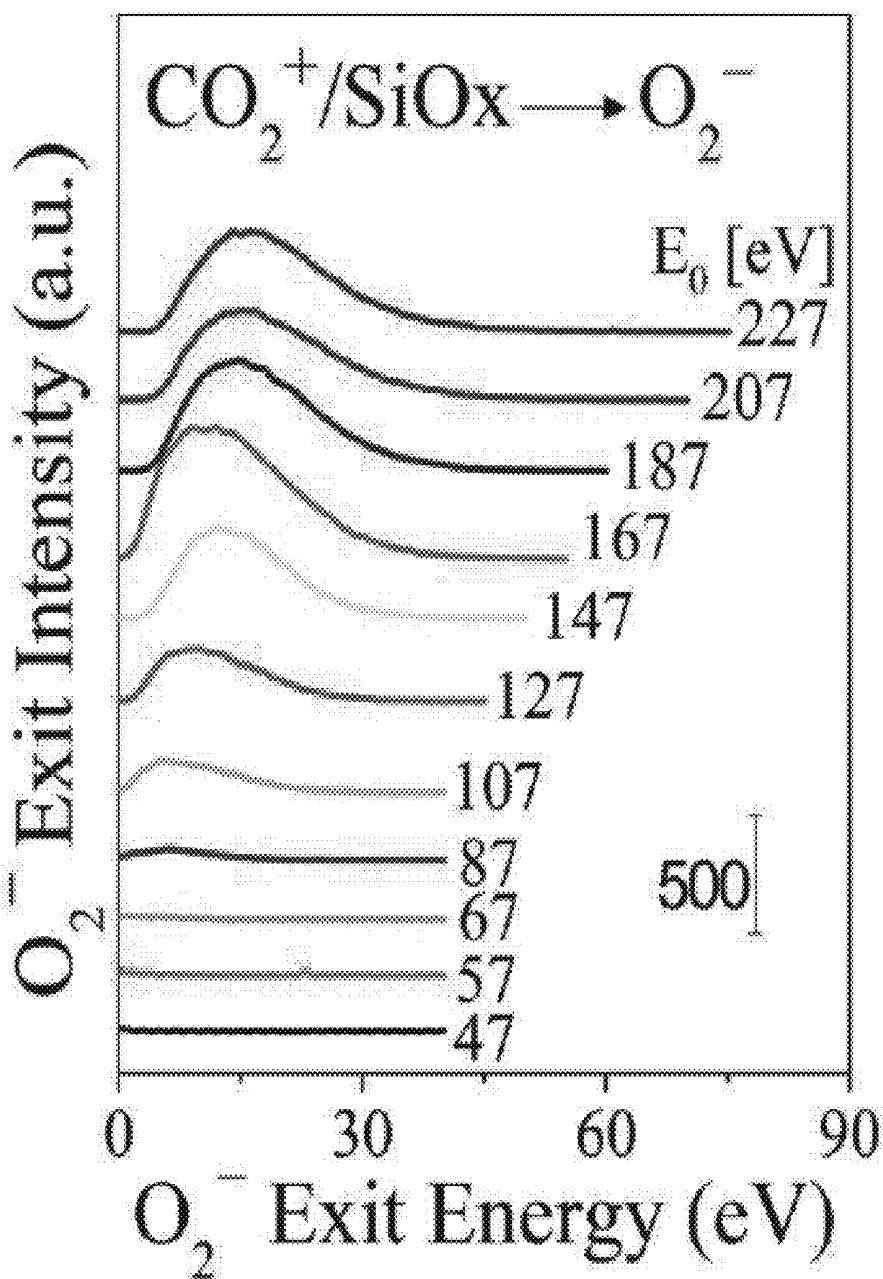
FIELD OF THE INVENTION

[0002] Apparatus and methods for producing molecular oxygen (or its relevant analogs, e.g., O_2^+ and O_2^- ions) directly from CO_2 molecules are provided.

BACKGROUND OF THE INVENTION

[0003] Carbon dioxide (CO_2) is a symmetric linear triatomic molecule, wherein carbon atom is covalently bound to two oxygen atoms via strong double bonds. Trace amounts of CO_2, a colorless gas, occur naturally in the Earth's atmosphere, wherein its current concentration is ~0.04% (405 ppm) by volume, having risen from pre-industrial levels of 280 ppm. However, despite a seemingly low concentration, CO_2 gas is the main contributor to the atmospheric greenhouse effect, and, therefore, is of major concern to humanity, especially in view of the alarmingly rapid increases of its atmospheric concentration in recent decades. Consequently, various technologies for CO_2 sequestration from the Earth's atmosphere are currently being investigated and pursued, although no definitive solution has been found to date.

[0004] In contrast, dioxygen gas (O_2) is the basis of life on Earth and is rather abundant in the atmosphere. However, an oxygen-rich atmosphere is quite unique to Earth, because, although elemental oxygen is the third most abundant element in the universe, its molecular dioxygen form is very rare. Specifically, in contrast to Earth, where oxygenic photosynthesis has made O_2 abundant, interstellar and cometary oxygen atoms are chemically bound to other elements in compounds such as H_2O, CO_2, CO, silicates, and metal oxides, making the release of O_2 from these reservoirs difficult and energetically very expensive. As such, only tenuous amounts of dioxygen are found elsewhere in our solar system, e.g., in the moons of Jupiter and Saturn and on Mars; in fact, the abundance of molecular oxygen has been suggested as a promising biomarker. Accordingly, efficient generation of O_2 from CO_2 is particularly desirable for space travel to Mars, Venus, and other planetary bodies with CO_2-rich atmospheres.

SUMMARY OF THE INVENTION

[0005] Embodiments are directed to methods and apparatus for forming molecule oxygen from carbon dioxide molecules.

[0006] In many embodiments the methods for splitting carbon dioxide into molecular oxygen and carbon include accelerating carbon dioxide molecules against a solid surface at an incident angle such that the carbon dioxide molecules have kinetic energy E_0 of between 10 and 300 eV at collision against the solid surface.

[0007] In other embodiments the method further includes accelerating the carbon dioxide molecules prior to the acceleration. In other such embodiments the carbon dioxide molecules are ionized by one of either photoexcitation or energetic electron bombardment.

[0008] In still other embodiments the accelerated carbon dioxide molecules have a kinetic energy of between 20 and 200 eV.

[0009] In yet other embodiments the carbon dioxide molecules subjected to acceleration are produced in a carbon dioxide plasma. In some such embodiments the plasma ionizes the carbon dioxide molecules to produce carbon dioxide ions, and wherein the potential of the plasma is externally adjusted to produce an electric field in the plasma such that the carbon dioxide ions are accelerated to the kinetic energy E_0.

[0010] In still yet other embodiments the solid surface comprises grounded metal electrodes.

[0011] In still yet other embodiments the solid surface comprises one or more element selected from the group: any element of rows 4, 5, and 6 of the Periodic table, an oxide of any element thereof, any combination thereof.

[0012] In still yet other embodiments the solid surface comprises one or more element selected from the group: Ti, V, Cr, Mn, Fe, CO, Ni, Cu, Zn, Ge, Y, Zr, Nb, Mo, Ru, Rh, Pd, Ag, In, Sn, Sb, Te, Ce, Hf, Ta, Re, Os, Ir, Pt, Au, Pb, Bi, an oxide of any element thereof, any combination thereof.

[0013] In still yet other embodiments the solid surface is selected from the group of silicon oxide or indium tin oxide.

[0014] In still yet other embodiments the acceleration occurs via application of an electric field.

[0015] In still yet other embodiments the conversion efficiency of carbon dioxide molecules to molecular oxygen is up to 33%.

[0016] In still yet other embodiments the conversion efficiency of carbon dioxide molecules to molecular oxygen is at least 5%.

[0017] Many other embodiments are directed to an apparatus for splitting carbon dioxide into molecular oxygen and carbon, including:

[0018] a source of a gaseous mixture comprising carbon dioxide gas,

[0019] a solid surface,

[0020] a molecular accelerator configured to selectively accelerate the carbon dioxide molecules against the solid surface at an incident angle, such that the kinetic energy of the carbon dioxide molecules at collision against the solid surface is between 10 and 300 eV.

[0021] In other embodiments the apparatus further includes an ionizer for ionizing the carbon dioxide molecules prior to the acceleration, and wherein the molecular accelerator comprises an electric field.

[0022] In still other embodiments the carbon dioxide molecules are ionized by one of either photoexcitation or energetic electron bombardment.

[0023] In yet other embodiments the accelerated carbon dioxide molecules have a kinetic energy of between 20 and 200 eV.

[0024] In still yet other embodiments the carbon dioxide molecules subjected to acceleration are produced in a carbon dioxide plasma. In some such embodiments the plasma ionizes the carbon dioxide molecules to produce carbon dioxide ions, and wherein the potential of the plasma is

externally adjusted to produce an electric field in the plasma such that the carbon dioxide ions are accelerated to the kinetic energy E_0.

[0025] In still yet other embodiments the solid surface comprises one or more grounded metal electrodes.

[0026] In still yet other embodiments the solid surface comprises one or more biased metal electrodes.

[0027] In still yet other embodiments the solid surface is selected form the group consisting of any element of rows 4, 5, and 6 of the Periodic table, an oxide of any element thereof, any combination thereof.

[0028] In still yet other embodiments the solid surface is selected form the group consisting of Ti, V, Cr, Mn, Fe, CO, Ni, Cu, Zn, Ge, Y, Zr, Nb, Mo, Ru, Rh, Pd, Ag, In, Sn, Sb, Te, Ce, Hf, Ta, Re, Os, Ir, Pt, Au, Pb, Bi, an oxide of any element thereof, any combination thereof.

[0029] In still yet other embodiments the solid surface is selected form the group of silicon oxide or indium tin oxide.

[0030] In still yet other embodiments the conversion efficiency of carbon dioxide molecules to molecular oxygen is up to 33%.

[0031] In still yet other embodiments the conversion efficiency of carbon dioxide molecules to molecular oxygen is at least 5%

[0032] Additional embodiments and features are set forth in part in the description that follows, and in part will become apparent to those skilled in the art upon examination of the specification or may be learned by the practice of the disclosed subject matter. A further understanding of the nature and advantages of the present disclosure may be realized by reference to the remaining portions of the specification and the drawings, which forms a part of this disclosure.

BRIEF DESCRIPTION OF THE DRAWINGS

[0033] These and other features and advantages of the present invention will be better understood by reference to the following detailed description when considered in conjunction with the accompanying data and figures, wherein:

[0034] FIGS. 1a-c summarize scattering dynamics of the three molecular ion products (CO_2^+ in FIG. 1a, O_2^+ in FIG. 1b, and O_2^- in FIG. 1c) resulting from CO_2^+ collisions with Au surface in accordance with embodiments of the application.

[0035] FIGS. 2a-d provide spectra confirming the presence of fragmentation products in CO_2^+ collisions with Au surface in accordance with embodiments of the application.

[0036] FIG. 3a schematically illustrates the collision sequence of an accelerated linear CO_2 molecule scattering on surface, in accordance with embodiments of the application. FIG. 3b provides data summarizing a kinematic analysis of the collision sequence depicted in FIG. 3a.

[0037] FIGS. 4a-b illustrate a velocity analysis (a) and estimation of the CO_2^* excitation energy (b) for scattered CO_2 dissociation products in accordance with embodiments of the application.

[0038] FIG. 5 provides data showing the trend in O_2 formation vs. partial dissociation in CO_2^+/Au collisions in accordance with embodiments of the application.

[0039] FIGS. 6a-c illustrate energy distributions of CO_2^+ (a), O_2^+ (b), and O_2^- (c) ion exits from CO_2^+/Pt collisions as a function of the respective product exit energy for various CO_2^+ beam energies (E_0), in accordance with embodiments of the application.

[0040] FIGS. 7a-d illustrate energy distributions of dissociation fragments from CO_2^+/Pt collisions, in accordance with embodiments of the application.

[0041] FIG. 8 illustrates energy distributions of O_2^- ions scattered from $CO_2^+/SiOx$ collisions, as a function of the CO_2^+ incidence energy, in accordance with embodiments of the application.

DETAILED DISCLOSURE

[0042] Turning to the drawings and data, methods and apparatus for the facile conversion of CO_2 to molecular oxygen are provided. It will be understood that the embodiments of the invention described herein are not intended to be exhaustive or to limit the invention to precise forms disclosed. Rather, the embodiments selected for description have been chosen to enable one skilled in the art to practice the invention.

[0043] Despite the pressing demand for effective removal of CO_2 from the atmosphere and apparent benefits of converting CO_2 specifically into O_2, only one abiotic pathway to O_2 was known until recently, namely, the three-body recombination reaction, $O+O+M\rightarrow O_2+M$, where the requisite atomic oxygen arises from CO_2 photo-dissociation and M is a third body (Kasting, J. F., Liu, S. C., Donahue, T. M. Oxygen levels in the prebiological atmosphere. *J. Geophys. Res.* 84, 3097-3107 (1979); and Segura, A., Measows, V. S., Kasting, J. F., Crisp, D., Cohen, M. Abiotic formation of O_2 and O_3 in high-CO_2 terrestrial atmospheres. *Astron. Astrophys.* 472, 665-679 (2007); the disclosures of which are incorporated herein by reference). This finding was superseded by the discovery of two new pathways for direct O_2 formation from CO_2: one via vacuum ultraviolet (VUV) photo-dissociation (as described in Lu, Z., Chang, Y. C., Yin, Q. Z., Ng, C. Y. & Jackson, W. M. Evidence for direct molecular oxygen production in CO_2 photodissociation. *Science* 346, 61-64 (2014), the disclosure of which is incorporated herein by reference) and one via dissociative electron attachment (DEA) (as described in Wang, X. D., Gao, X. F., Xuan, C. J. & Tian, S. X. Dissociative electron attachment to CO_2 produces molecular oxygen. *Nature Chem.* 8, 258-263 (2016), the disclosure of which is incorporated herein by reference). In both of these latter studies, direct detection of the neutral O_2 photoproduct was not possible because of background interference. Instead, experimental evidence for the dissociation reaction of a highly-excited CO_2 electronic state (Suits, A. G. & Parker, D. H. Hot molecules-off the batten path. *Science* 346, 30 (2014), the disclosure of which is incorporated herein by reference) into the $C(^3P)+O_2$ ($X^3\Sigma_g^-$) products was based on detecting the complementary atomic C^+ or C^- fragment. In addition, O_2^+ ions from the photo-dissociation of CO_2 were recently detected using strong laser fields to photo-produce the doubly-ionized CO_2^{++} state, which dissociates into $C^++O_2^+$, altogether a very inefficient process (Larimian, S. et al. Molecular oxygen observed by direct photoproduction from carbon dioxide. *Phys. Rev. A* 95, 011404 (2017), the disclosure of which is incorporated herein by reference). Direct production of O_2^- from dissociative attachment in CO_2 has collision cross sections so small (~10^{-24} cm^2) that "signal must be accumulated over several days" to observe it even with extremely sensitive detection systems (Spence, D. & Schulz, G. J. Cross sections for production of O_2^- and C by dissociative electron attachment in CO_2: an observation of the Renner-Teller effect. *J. Chem. Phys.* 60, 216-220 (1974), the

disclosure of which is incorporated herein by reference). Therefore, new methods for the efficient splitting of CO_2 to produce O_2 are highly desirable and sought after in areas ranging from atmospheric science to space travel.

[0044] Direct conversion of CO_2 into molecular oxygen is an energetically very unfavorable reaction. In principle, direct dissociation of CO_2 can proceed along three pathways (shown below with the indicated dissociation energies):

$$CO_2 \rightarrow CO + O \text{ (5.5 eV)} \tag{I}$$

$$CO_2 \rightarrow C + O_2 \text{ (5.8 eV)} \tag{II}$$

$$CO_2 \rightarrow C + 2O \text{ (11.0 eV)} \tag{III}$$

Channel (I) describes the primary partial dissociation reaction, which has been widely studied in photochemistry and in heterogeneous catalysis under thermal activation conditions (as detailed, for example, in: Rosen, B. A. et al. Ionic liquid-mediated selective conversion of CO_2 to CO at low overpotentials. *Science* 334, 643-644 (2011); and Liu, M. et al. Enhanced electrocatalytic CO_2 reduction via field-induced reagent concentration. *Nature* 537, 382-386 (2016), the disclosures of which are incorporated herein by reference). Channel (III) represents the energetically expensive complete dissociation of CO_2 with cleavage of both C—O bonds. In contrast, channel (II) is an exotic pathway, which requires extensive intramolecular bond rearrangement within the triatomic CO_2, despite the fact that its dissociation energy is only 0.3 eV larger than that of channel (I). However, simulations have shown a possible way to realize channel (II) by first forming the cyclic CO_2 complex [c-CO_2 ($^1A_1$)], which then must transform into the collinear COO ($^1\Sigma^+$) intermediate on its way to dissociation into C+O_2. The first step in this scheme requires bending of the linear CO_2 molecule in order to bring the two O atoms in close proximity. Although inaccessible by thermal activation, the barrier to bending may be, in theory, overcome by other means of excitation, such as VUV photon irradiation or energetic electron bombardment.

[0045] It has now been discovered that, as described in the embodiments of this invention, channel (II) can also be activated by energetic collisions of CO_2 molecules (or, in some embodiments, of their CO_2^+ ion analogs) with solid surfaces. In many such embodiments, when CO_2^+ ions are collided with a solid surface, O_2 molecules and $O_2^\pm$ ions evolve directly from a scattered excited state (CO_2^*) undergoing late fragmentation. Accordingly, this application is directed to embodiments of an unexpected and surprisingly efficient method for facilitating an intramolecular reaction that occurs in single collisions of CO_2 molecules (or their derivatives amenable to controllable acceleration, such as CO_2^+ ions) with a solid surface, such that molecular oxygen (or its relevant analogs, e.g., O_2^+ and O_2^- ions) is directly produced. In many embodiments of the invention, the reaction is driven by momentum of the CO_2 molecule or ion accelerated against a surface and incoming at an incident angle and will occur irrespective of the surface composition and temperature. However, in many embodiments, the yield of O_2 production from CO_2 splitting does depend on surface composition in so far as surfaces that would be reactive with CO_2 or its fragmentation products can poison the reaction. In some embodiments, the method may be used to remove CO_2 from Earth's atmosphere, while, in other embodiments, the method may be used to prevent the atmosphere's contamination with CO_2 emissions. In yet other embodiments, the

method may be used to obtain molecular oxygen in CO_2-rich environments, such as to facilitate exploration of extraterrestrial bodies with CO_2-rich atmospheres (e.g. Mars).

[0046] In many embodiments, the method for splitting carbon dioxide into molecular oxygen and carbon comprises accelerating molecules of CO_2 to a specific desired velocity, such that the accelerated molecules collide with a solid surface with kinetic energies between 10 and 300 eV. It will be understood that, within this kinetic energy range, the actual amount of energy required for the optimum conversion to O_2 is determined by such parameters as the angle at which the accelerated CO_2 molecule or ion approaches the surface prior to the collision and the atomic mass of the surface atoms. In many embodiments, larger kinetic energies are required to facilitate the reaction for larger angles of incidence θ with respect to the surface normal vector, wherein the least amount of required energy corresponds to normal incidence. More specifically, in many embodiments, if E_0 is the required kinetic energy for maximum conversion at an angle of incidence θ, then the corresponding energy for normal incidence would be $E_0 \cos^2 \theta$.

[0047] Without being bound by any theory, the kinematic analysis of the collisional process suggests that CO_2 collisions with the provided surface under the disclosed herein conditions extensively perturb the CO_2 intramolecular triatomic geometry and produce a strongly bent CO_2 excited state, which, subsequently, dissociates to yield molecular as well as ionized O_2. The disclosed herein process is reminiscent of exotic photochemical pathways for CO_2 decomposition, but, unlike any known pathway, which typically have very low O_2 yields, the intramolecular CO_2 decomposition conducted according to the embodiments of this invention has an estimated O_2 yield of ~33±3%. For comparison, the yield of previously reported CO_2 photo-dissociation pathways is ~5±2%.

[0048] Of course, it will be understood that any acceleration technique known in the art can be employed to bring CO_2 molecules to the velocities and surface striking energies necessary to enable the method of this application. Several approaches are known in the art to produce positively charged CO_2 ions and to controllably accelerate them with an applied electric field. Accordingly, in many embodiments, prior to acceleration, the CO_2 molecules are ionized via photo-excitation with ultraviolet light. In some other embodiments, the CO_2 molecules are ionized by means of energetic electron bombardment under low pressure. In yet other, preferred embodiments, CO_2 plasma is used to produce CO_2^+, which are accelerated against a biased surface with appropriate energy. In yet another embodiment, the solid surface may be moving against heated CO_2 molecules at the required velocity.

[0049] In many embodiments, O_2 ions are directly produced in hyperthermal CO_2^+ collisions against Au surfaces. Specifically, FIGS. 1a to 1c summarize exemplary scattering dynamics of such CO_2^+/surface collisions, by showing energy distributions for three of its molecular ion products: CO_2^+ (FIG. 1a), O_2^+ (FIG. 1b), and O_2^- (FIG. 1c) for various CO_2^+ beam energies (E_0) (as annotated on each panel), and shows that both O_2 ions are detected at certain, relatively narrow energy ranges, along with some amount of survived CO_2^+. Accordingly, first, FIG. 1a shows that a very weak scattered CO_2^+ signal is detected at beam energies (E_0) below 100 eV. Furthermore, the scattered CO_2^+ ion exit energy varies in proportion to the CO_2^+ incidence energy,

thus precluding physical sputtering as its origin. Observing dynamic CO_2^+ signal is important because it proves that some CO_2 survives the collision. In addition, the observed kinematics provide insight into the collision sequence of the constituent atoms of the triatomic molecule impinging onto the metal surface. Second, in FIGS. 1b and 1c a strong scattered O_2 signal is observed in both charge polarities, O_2^+ and O_2^-. Here, in contrast to the O_2^- energy spectra, the O_2^+ signal appears somewhat noisy, owing to detector (channeltron) operation. As observed for the scattered CO_2^+, the O_2^+ and O_2^- ion exit energies increase monotonically with the CO_2^+ incidence energy. For both polarities, the scattered O_2 ion signal intensity goes through a maximum, then it dies out for $E_0 > 150$ eV. Interestingly, the O_2^+ energy spectra develop a shoulder at ~20 eV for beam energies greater than 100 eV due to physical sputtering. As noted above, the O_2^+ and O_2^- spectra intensities cannot be directly compared due to differences in how the detector is biased.

[0050] Notably, the demonstrated O_2 formation is unexpected, since collision-induced dissociation of CO_2^+ is expected to occur via channel (I) at low collision energies, followed up by channel (III) at larger incidence energies. Indeed, FIGS. 2a-d show that all of the CO_2^+ dissociation products: CO^+, O^+, O^-, and C^+, are detected in CO_2^+/Au collisions. Furthermore, the exit energies of the CO^+ and O^- peaks vary with incidence energy (FIGS. 2a and 2c), indicating they are produced dynamically within the surface collision. However, as will be shown below, these fragments originate from the same excited state as the one producing the O_2 ions. In contrast, the position of the O^+ and C^+ peaks is almost invariant around 20 eV (Exit Energy), suggesting a different origin. The appearance of scattered C^+ products for $E_0 > 70$ eV confirms that complete dissociation of CO_2 via channel (III) also occurs.

[0051] Since scattered CO_2^+ ions are detected along with other collision products, a fraction of the incident ions must survive the hard collision. The kinematics (described in Yao, Y. & Giapis, K. P. Kinematics of Eley-Rideal reactions at hyperthermal energies. *Phys. Rev. Lett.* 116, 253202 (2016), the disclosure of which is incorporated herein by reference) of the scattered CO_2^+ ions can help elucidate the scattering mechanism, which in turn provides clues for the formation of O_2. Accordingly, FIG. 3a schematically illustrates the collision sequence of a linear CO_2 molecule scattering on a solid surface according to many embodiments of this invention. In this scheme, the leading O atom collides with the surface first, followed by collision of the complementary CO moiety, and further followed by the molecule bending during the hard collision and forming of an excited triangular state, which, in turn, undergoes late dissociation into $C+O_2$.

[0052] FIG. 3b provides ion exit energies of CO_2^+, O_2^+, O_2^-, CO^+, O^-, and C^+ ions as a function of CO_2^+ incidence energy, along with corresponding one-parameter linear fittings as solid lines. Here, the slope for CO_2^+ is calculated from binary collision theory (BCT), assuming two sequential collisions as proposed in the scheme depicted in FIG. 3a; while the other slopes are calculated by assuming a common excited CO_2 precursor state fragmenting spontaneously into daughter ions. It should be noted, that since the O_2^+ exit energy data overlaps with the O_2 data, only the linear fitting for O_2^- is shown in FIG. 3b. In view of the data presented in FIG. 3b, first, if CO_2^+ scatters as a whole molecule (i.e., a hard sphere with atomic mass of 44 Dalton), BCT predicts a kinematic factor of 0.6349, which does not fit well the

energy data shown in FIG. 3b. This is not surprising given the quasi-linear triatomic nature of the CO_2^+ ion (as explained in Walsh, A. D. The electronic orbitals, shapes, and spectra of polyatomic molecules. Part II. Non-hydride AB_2 and BAC molecules *J. Chem. Soc.,* 2266-2288 (1953); and Grimm, F. A. & Larsson, M. A Theoretical Investigation of the Low Lying Electronic States of CO_2^+ in Both Linear and Bent Configurations. *Phys. Scr.* 29, 337-343 (1984); the disclosures of which are incorporated herein by reference). The next plausible scattering model assumes that parts of the molecular ion suffer distinct and successive collisions without molecular dissociation (as depicted in FIG. 3a): first the leading O atom collides with a surface Au atom, then the remaining CO moiety collides with the same Au atom. This model is similar to how diatomic molecules scatter on metal surfaces (as described, for example in Yao, Y. & Giapis, K. P. Direct hydrogenation of dinitrogen and dioxygen via Eley-Rideal reactions. *Angew. Chem. Int. Ed.* 55, 11595-11599 (2016), the disclosure of which is incorporated herein by reference). Applying BCT to the sequential collision scattering model yields a kinematic factor of 0.7870, which fits perfectly the CO_2^+ exit energy data provided in FIG. 3b. This scattering behavior has been verified for another quasi-linear molecular ion, NO_2^+, when scattering on Au surfaces (described in Pfeiffer, G. V. & Allen, L. Electronic structure and geometry of NO_2^+ and NO_2^-. *J. Chem. Phys.* 51, 190-202 (1969), the disclosure of which is incorporated herein by reference).

[0053] Accordingly, in many embodiments, facilitating energetic CO_2^+ scattering against a biased surface affects the angular configuration of the CO_2 molecule during the collision and results in the unexpectedly efficient O_2 production. Although not to be bound by theory, according to the disclosed herein mechanism and for many CO_2 approach geometries, one of the O atoms of the CO_2 molecule collides with the surface first and then rebounds in closer proximity to the other O atom in the resulting CO moiety. This mechanical deformation of the CO_2 molecule is equivalent to a bending mode but occurs at much faster timescales than vibronic interactions (Renner-Teller effect). In addition, electronic excitation may also occur during the hard collision (as explained in Mace, J., Gordon, M. J. & Giapis, K. P. Evidence of simultaneous double-electron promotion in F+ collisions with surfaces. *Phys. Rev. Lett.* 97, 257603 (2006), the disclosure of which is incorporated herein by reference). Therefore, according to many embodiments, a strongly bent, highly excited CO_2^* state is produced in CO_2/surface collision, which next decomposes preferentially into $C+O_2$ on the rebound from the surface. Furthermore, in some embodiments, charge exchange of the CO_2 dissociation fragments with the surface may aide the ionization of the O_2 (FIG. 3a). In other embodiments, the excited state may split directly into ion pairs.

[0054] Furthermore, the very weak signal observed for CO_2^+ scattered according to the embodiments of the invention implies a very low survival probability. CO_2^+ fragmentation can occur before, during, or after the hard collision with the surface. Only delayed fragmentation, for example, of a rebounding highly excited CO_2^* precursor state, can explain dissociation products having the same exit velocity as the precursor. Therefore, according to some embodiments, the kinematic factors of O_2, CO and O products can be calculated from energy conservation to be 0.5724, 0.5008, and 0.2862, respectively. The linear O_2^-, CO^+ and

O⁻ ion exit data are fitted very well with these kinematic factors as slopes (FIG. 3b). However, the O_+ and C^+ data cannot be fitted linearly, wherein their broader distributions suggest that other processes, such as surface sputtering, contribute to the measured peaks at lower energies, rendering de-convolution of the contribution from excited CO_2* difficult.

[0055] According to many embodiments and the observed kinematics of the ion exits from CO_2^+ scattering on Au, molecular O_2 ions originate in surviving CO_2 molecules or ions, possibly highly excited. To further illustrate this process, the distributions of the CO_2^+, O_2^+, O_2^-, CO^+ and O^- ion exits for $E_0=56.4$ eV are re-plotted in FIG. 4a as a function of the corresponding ion exit velocity. As seen in FIG. 4a, the exit velocities of scattered CO^+, O_2^+ and O_2^- line up very well, thus confirming the single precursor origin, while the O^- peak is somewhat broader than the latter three and overlaps partially with the O_2 ion exit peaks. Surprisingly, the surviving CO_2^+ is clearly faster than the O_2 ion products. Therefore, the CO_2* undergoing post-collisional dissociation according to the embodiments of the invention must become internally excited by inelastic processes, which, in turn, robs kinetic energy from the incident CO_2^+ and results in its slower exit. Although the putative CO_2* state cannot be directly detected, the additional energy needed to produce it can be estimated by assuming that the daughter O_2^- ion is emitted with the CO_2* exit velocity. Then, the kinetic energy difference between CO_2^+ and CO_2* can be estimated and should be a measure of the relative excitation energy. Accordingly, FIG. 4b summarizes the results of this simple calculation as a function of E_0. Notably, for $E_0<70$ eV, the relative excitation energy is about 6 eV—a value remarkably close to that required for CO_2 partial dissociation according to channel (I) mechanism, or for direct O_2 formation according to channel (II) mechanism. Coincidentally, the energy penalty to form the triangular CO_2 state ($^1A_1$) is also 6 eV (as reported in Lu, Z., Chang, Y. C., Yin, Q. Z., Ng, C. Y. & Jackson, W. M. Evidence for direct molecular oxygen production in CO_2 photodissociation, *Science* 346, 61-64 (2014), the disclosure of which is incorporated herein by reference). For E_0 above 70 eV, the relative excitation energy increases while the scattered CO_2^+ signal dies out (FIG. 1a). Simultaneously, C^+ ions become detectable suggesting the onset of complete dissociation via channel (Ill).

[0056] Due to the violence of the surface collision, even the surviving CO_2 molecular ions can be highly excited. The intercept of the CO_2^+ data fitting in FIG. 3b reflects the inelastic energy loss for the CO_2^+ ion exit, which amounts to 8.69 eV—most of it going to internal excitation. Adding the inelastic energy loss of the surviving CO_2^+, the absolute excitation energy for the CO_2* precursor could be as high as 14 eV. This energy is comparable to the VUV-photon and electron energy needed for the direct formation of O_2 from CO_2.

[0057] An important question for the CO_2^+ dissociation reaction into O_2 is that of efficiency. One way to assess the efficiency of CO_2 dissociation according to the embodiments of the application is in terms of selectivity of channel (II) versus the predominant channel (I). Kinematic analysis has shown that the CO^+, O_2^- and O^- products are directly formed from a common parent, the putative CO_2* excited precursor state. At low CO_2^+ incidence energies, the main dissociation pathways are: a) partial dissociation to form

CO+O (channel (I)), and b) intramolecular reaction to form O_2+C (channel (II)). Assuming that O_2^- and O^- are formed by resonant electron transfer to the corresponding neutrals with the same efficiency, one can use the relative intensity of O_2^- and O^- to estimate the selectivity for O_2 formation, $S(O_2)$, defined as follows:

$$S(O_2) = \frac{I(O_2^-)}{I(O_2^-)+I(O^-)},$$

where I is the intensity of the corresponding negative ion exits. Notably, the electron affinities of O atoms and O_2 are 1.46 eV and 0.45 eV, respectively, wherein the difference implies that negative ion formation should be more efficient for 0 than for O_2, due to the lower barrier to resonant electron attachment. Therefore, $S(O_2)$, as defined here, underestimates the actual O_2 formation selectivity. Furthermore, at high CO_2^+ incidence energy, channel (III) also opens up, doubling the number of O atoms and O^- ions produced and, thus, further worsening the estimate for O_2 formation selectivity. With these limitations in mind, one can obtain a conservative estimate of the O_2 formation selectivity, which is plotted in FIG. 5 as a function of CO_2^+ incidence energy. According to the data plotted in FIG. 5, the O_2 formation selectivity increases with E_0, goes through a maximum of ~33±3% at $E_0=70$ eV, then decreases. The first increase is consistent with more energy available for direct O_2 formation. Remarkably, the turnaround point coincides with the opening up of the complete dissociation channel.

[0058] Although the above discussed results are based on monitoring ionic products, it is well known in ion-surface collisions, that the majority (~98%) of the ions are neutralized by the surface prior to the collision and thus collide with the surface as neutrals, in this case neutral (uncharged) CO_2. Likewise, many scattered CO_2 molecules and products of CO_2 dissociation will not be charged, nevertheless will be contributing to the O_2 yield.

[0059] The direct O_2 production by collisional activation of CO_2^+ according to the embodiments of the application is clearly more efficient than activation using other means, such as high-energy photons or electrons. Indeed, O_2 formation by photo-excitation of CO_2 has an estimated selectivity of only 5±2% vs. the partial dissociation channel, while DEA processes in CO_2 have minuscule cross sections for O_2 production. In many embodiments, the higher O_2 selectivity in the collisional activation process is attributed to more facile structural rearrangement in the CO_2 during the hard collision, which brings the two O atoms closer together.

[0060] In some embodiments, the atomic composition of the collision surface affects the O_2 yield of CO_2 splitting method of the application and must be optimized. Specifically, in many embodiments, surfaces that can be easily sputtered, i.e., where the surface erodes significantly at low incidence energy, or where carbon atoms stick preferentially to the surface to form coatings, are not desirable, as they can interfere with the surface excitation process that facilitates the reaction and poison the CO_2 dissociation. Consequently, in many embodiments, the general requirement for the collision surface is that it contains an atom with atomic mass larger than 16-18 Dalton, which is the atomic mass of the elemental oxygen, including its isotopes. In many preferred embodiments, the atomic mass of the collision surface elements is between 20 and 200 Dalton. Furthermore,

although surfaces comprising atoms with atomic mass larger than 20 Dalton are acceptable, surfaces comprising atoms with atomic mass heavier than 40 Dalton are preferred. In many embodiments, the collision surface comprises of one or more element found in rows 4, 5, and 6 of the Periodic table or such element's oxide. In some such embodiments, the collision surface is comprised of one or more element from the list: Ti, V, Cr, Mn, Fe, CO, Ni, Cu, Zn, Ge, Y, Zr, Nb, Mo, Ru, Rh, Pd, Ag, In, Sn, Sb, Te, Ce, Hf, Ta, Re, Os, Ir, Pt, Au, Pb, Bi, an oxide of any element thereof, or any combination thereof. In contrast, in many embodiments, surfaces comprising certain elements that might interfere with the CO_2 dissociation reaction must be avoided. For example, surfaces comprising tungsten (W) must be avoided in many embodiments, as such surfaces, when oxidized, form a volatile tungsten oxide that vaporizes and consumes the surface.

[0061] Furthermore, in many embodiments, the collision enabled CO_2 splitting reaction is generic to metal surfaces (FIGS. 6 and 7), and occurs even on oxides (FIG. 8). Specifically, FIGS. 6 and 7 demonstrate that, in some embodiments, efficient splitting of CO_2 into O_2 can be achieved via CO_2 collisions with Pt surfaces, while FIG. 8 shows that, in other embodiments, the similar behavior is observed in CO_2 collisions with silicon oxide surfaces.

[0062] In many embodiments, the CO_2 splitting method of the instant application may be exploited in plasma reactors, wherein ion/wall collisions occur spontaneously at energies determined by the plasma potential. Remarkably, past attempts at using CO_2 plasmas were plugged by relatively low O_2 conversion, ostensibly because of the slow kinetics for the two-step O_2 formation process in gas-phase collisions (as detailed in Spencer, L. F. & Gallimore, A. D. Efficiency of CO_2 dissociation in a radio-frequency discharge. *Plasma Chem. Plasma Phys.* 31, 79-89 (2010), the disclosure of which is incorporated herein by reference). However, according to the embodiments of the invention, the O_2 yield is greatly improved with the following three modifications to plasma reactor methods of CO_2 splitting: a) maximizing the CO_2^+ ion density, b) tuning the plasma potential between 40 and 150 eV, and c) providing grounded metal electrodes to enable CO_2^+ ion/surface collisions.

Exemplary Embodiments/Experimental Materials and Methods

[0063] The following example sets forth certain selected embodiments relate to the above disclosure. It will be understood that the embodiments presented in this section are exemplary in nature and are provided to support and extend the broader disclosure, these embodiments are not meant to confine or otherwise limit the scope of the invention.

[0064] All experiments described in the instant application were carried out in a custom-made low-energy ion scattering apparatus described in detail in Gordon, M. J. & Giapis, K. P. Low-energy ion beam line scattering apparatus for surface science investigations. *Rev. Sci. Instrum.* 76, 083302 (2005), the disclosure of which is incorporated herein by reference. The CO_2^+ ion beam was extracted from an inductively-coupled plasma, struck in a reactor held at 2 mTorr using a CO_2/Ar/Ne gas mixture supplied with 500 W RF power at 13.56 MHz. Ions delivered to a grounded surface at 45° incidence angle; typical beam currents of 5 to 15 μA were spread over a ~3 mm spot. Beam energy was varied between

40-200 eV by externally adjusting the plasma potential. Typical target surfaces were polycrystalline Au foils (5N), sputter-cleaned with an Ar+ ion gun before each run. Scattered ion products, exiting at an angle of 45° in the scattering plane, were energy- and mass-resolved using an electrostatic ion energy analyzer and a quadruple mass spectrometer, respectively. All ions were detected using a channel electron multiplier, biased as appropriate to detect positive or negative ions. Differences in detector bias precluded a direct comparison of signal intensities between product ions of different charge polarities. All collected signals were normalized to the beam current measured on the sample.

DOCTRINE OF EQUIVALENTS

[0065] This description of the invention has been presented for the purposes of illustration and description. It is not intended to be exhaustive or to limit the invention to the precise form described, and many modifications and variations are possible in light of the teaching above. The embodiments were chosen and described in order to best explain the principles of the invention and its practical applications. This description will enable others skilled in the art to best utilize and practice the invention in various embodiments and with various modifications as are suited to a particular use. The scope of the invention is defined by the following claims.

1. A method for splitting carbon dioxide into molecular oxygen and carbon, comprising accelerating carbon dioxide molecules against a solid surface at an incident angle such that the carbon dioxide molecules have kinetic energy E_0 of between 10 and 300 eV at collision against the solid surface.

2. The method of claim 1, further comprising ionizing the carbon dioxide molecules prior to the acceleration.

3. The method of claim 2, wherein the carbon dioxide molecules are ionized by one of either photoexcitation or energetic electron bombardment.

4. The method of claim 1, wherein the accelerated carbon dioxide molecules have a kinetic energy of between 20 and 200 eV.

5. The method of claim 1, wherein the carbon dioxide molecules subjected to acceleration are produced in a carbon dioxide plasma.

6. The method of claim 5, wherein the plasma ionizes the carbon dioxide molecules to produce carbon dioxide ions, and wherein the potential of the plasma is externally adjusted to produce an electric field in the plasma such that the carbon dioxide ions are accelerated to the kinetic energy E_0.

7. The method of claim 1, wherein the solid surface comprises grounded metal electrodes.

8. The method of claim 1, wherein the solid surface comprises one or more element selected from the group: any element of rows 4, 5, and 6 of the Periodic table, an oxide of any element thereof, any combination thereof.

9. The method of claim 1, wherein the solid surface comprises one or more element selected from the group: Ti, V, Cr, Mn, Fe, CO, Ni, Cu, Zn, Ge, Y, Zr, Nb, Mo, Ru, Rh, Pd, Ag, In, Sn, Sb, Te, Ce, Hf, Ta, Re, Os, Ir, Pt, Au, Pb, Bi, an oxide of any element thereof, any combination thereof.

10. The method of claim 1, wherein the solid surface is selected from the group of silicon oxide or indium tin oxide.

11. The method of claim 1, wherein the acceleration occurs via application of an electric field.

12. The method of claim 1, wherein the conversion efficiency of carbon dioxide molecules to molecular oxygen is up to 33%.

13. The method of claim 1, wherein the conversion efficiency of carbon dioxide molecules to molecular oxygen is at least 5%.

14. An apparatus for splitting carbon dioxide into molecular oxygen and carbon, comprising:
  a source of a gaseous mixture comprising carbon dioxide gas,
  a solid surface,
  a molecular accelerator configured to selectively accelerate the carbon dioxide molecules against the solid surface at an incident angle, such that the kinetic energy of the carbon dioxide molecules at collision against the solid surface is between 10 and 300 eV.

15. The apparatus of claim 11, further comprising an ionizer for ionizing the carbon dioxide molecules prior to the acceleration, and wherein the molecular accelerator comprises an electric field.

16. The apparatus of claim 12, wherein the carbon dioxide molecules are ionized by one of either photoexcitation or energetic electron bombardment.

17. The apparatus of claim 11, wherein the accelerated carbon dioxide molecules have a kinetic energy of between 20 and 200 eV.

18. The apparatus of claim 11, wherein the carbon dioxide molecules subjected to acceleration are produced in a carbon dioxide plasma.

19. The apparatus of claim 15, wherein the plasma ionizes the carbon dioxide molecules to produce carbon dioxide ions, and wherein the potential of the plasma is externally adjusted to produce an electric field in the plasma such that the carbon dioxide ions are accelerated to the kinetic energy E_0.

20. The apparatus of claim 11, wherein the solid surface comprises one or more grounded metal electrodes.

21. The apparatus of claim 11, wherein the solid surface comprises one or more biased metal electrodes.

22. The apparatus of claim 11, wherein the solid surface is selected form the group consisting of any element of rows 4, 5, and 6 of the Periodic table, an oxide of any element thereof, any combination thereof.

23. The apparatus of claim 11, wherein the solid surface is selected form the group consisting of Ti, V, Cr, Mn, Fe, CO, Ni, Cu, Zn, Ge, Y, Zr, Nb, Mo, Ru, Rh, Pd, Ag, In, Sn, Sb, Te, Ce, Hf, Ta, Re, Os, Ir, Pt, Au, Pb, Bi, an oxide of any element thereof, any combination thereof.

24. The apparatus of claim 11, wherein the solid surface is selected form the group of silicon oxide or indium tin oxide.

25. The apparatus of claim 11, wherein the conversion efficiency of carbon dioxide molecules to molecular oxygen is up to 33%.

26. The apparatus of claim 11, wherein the conversion efficiency of carbon dioxide molecules to molecular oxygen is at least 5%.

* * * * *